Site-specific vibrational dynamics of the CD3ζ membrane peptide using heterodyned two-dimensional infrared photon echo spectroscopy

Prabuddha Mukherjee, Amber T. Krummel, Eric C. Fulmer, Itamar Kass, Isaiah T. Arkin, and Martin T. Zanni

Articles you may be interested in

Influence of temperature on thymine-to-solvent vibrational energy transfer
J. Chem. Phys. **135**, 114505 (2011); 10.1063/1.3628451

Probing intermolecular couplings in liquid water with two-dimensional infrared photon echo spectroscopy
J. Chem. Phys. **128**, 191103 (2008); 10.1063/1.2919050

Coupling and orientation between anharmonic vibrations characterized with two-dimensional infrared vibrational echo spectroscopy
J. Chem. Phys. **115**, 10814 (2001); 10.1063/1.1417504

Two-dimensional heterodyned and stimulated infrared photon echoes of N-methylacetamide-D
J. Chem. Phys. **114**, 4579 (2001); 10.1063/1.1346647

APL Photonics

Site-specific vibrational dynamics of the CD3ζ membrane peptide using heterodyned two-dimensional infrared photon echo spectroscopy

Prabuddha Mukherjee, Amber T. Krummel, and Eric C. Fulmer
Department of Chemistry, University of Wisconsin—Madison, Madison, Wisconsin 53706

Itamar Kass and Isaiah T. Arkin
The Alexander Silberman Institute of Life Sciences, Department of Biological Chemistry, The Hebrew University, Givat-Ram, Jerusalem, 91904 Israel

Martin T. Zanni[a]
Department of Chemistry, University of Wisconsin—Madison, Madison, Wisconsin 53706

Heterodyned two-dimensional infrared (2D IR) spectroscopy has been used to study the amide I vibrational dynamics of a 27-residue peptide in lipid vesicles that encompasses the transmembrane domain of the T-cell receptor CD3ζ. Using $1-{}^{13}C={}^{18}O$ isotope labeling, the amide I mode of the 49-Leucine residue was spectroscopically isolated and the homogeneous and inhomogeneous linewidths of this mode were measured by fitting the 2D IR spectrum collected with a photon echo pulse sequence. The pure dephasing and inhomogeneous linewidths are 2 and 32 cm^{-1}, respectively. The population relaxation time of the amide I band was measured with a transient grating, and it contributes 9 cm^{-1} to the linewidth. Comparison of the 49-Leucine amide I mode and the amide I band of the entire CD3ζ peptide reveals that the vibrational dynamics are not uniform along the length of the peptide. Possible origins for the large amount of inhomogeneity present at the 49-Leucine site are discussed. © *2004 American Institute of Physics.* [DOI: 10.1063/1.1718332]

I. INTRODUCTION

Infrared photon echoes and two-dimensional infrared (2D IR) spectroscopy have now been used to probe the structures and dynamics of small molecules,[1–3] liquids,[4–7] soluble peptides,[8–12] and DNA.[13] In 2D IR spectroscopy, the intensities and splittings of the diagonal and cross peaks provide the anharmonities of the potential surface. The anharmonicities are sensitive to the molecular structure because they are caused by coupling between molecular vibrational modes and thus provide structural information.[9,14–16] Furthermore, the 2D line shapes of the peaks contain information on the distribution of select eigenstates, the frequency fluctuations caused by solvent and structural dynamics,[17–19] and the correlation between the vibrational modes.[20–23] Thus a precise understanding of the couplings and line shapes provides information on the structure and environment of the system. In this paper, we focus on characterizing the amide I line shape of the CD3ζ transmembrane peptide, reconstituted in membrane vesicles using $1-{}^{13}C={}^{18}O$ isotope labeling and 2D IR photon echo spectroscopy. We are interested in understanding how the frequency fluctuations that determine the amide I line shape are correlated to the fluctuations in the peptide structure and its heterogeneous membrane environment.

The line shapes of vibrational modes are caused by dephasing and population relaxation.[24,25] Dephasing is the result of a static and/or dynamic environment around the vibrational mode that subsequently alters the potential energy surface of the vibrator and hence its frequency. Fluctuations in hydrogen bonding and electrostatics are common sources of dephasing, which occur, for example, because of fluctuations in the structures of the molecule or solvent around the vibrational mode. As a result, the dephasing time of vibrational modes is a sensitive indicator of the environment around that mode.

When the frequency fluctuations that cause dephasing are static, the system is inhomogeneously broadened and the line shape reflects the distribution of environments. In the Kubo model, this limit leads to a Gaussian line in the linear infrared spectrum.[24] If the motions are instead very rapid, the system is homogeneously broadened and the line shape becomes a Lorentzian. In general, the dynamics is more complicated. For example, the time scale might be between these two limits or might decay on several time scales, in which case the line shape is neither Gaussian nor Lorentzian and linear infrared spectroscopy becomes insensitive to the dynamics. However, infrared photon echo spectroscopy is sensitive to the dynamics of the frequency fluctuations and can be used to extract the frequency–frequency correlation function that precisely describes the dephasing.[26] In photon echo 2D IR spectroscopy, the slow fluctuations can be removed from one axis in the 2D IR spectra by rephasing the coherence created by the first laser pulse, and the resulting 2D line shape reveals the homogeneous and inhomogeneous widths.[17,27] By waiting a time before rephasing the coherences, stimulated photon echoes monitor the time dependence of the inhomogeneous distribution from which the correlation function is extracted.[28]

---
[a]Author to whom correspondence should be addressed. Electronic mail: zanni@chem.wisc.edu
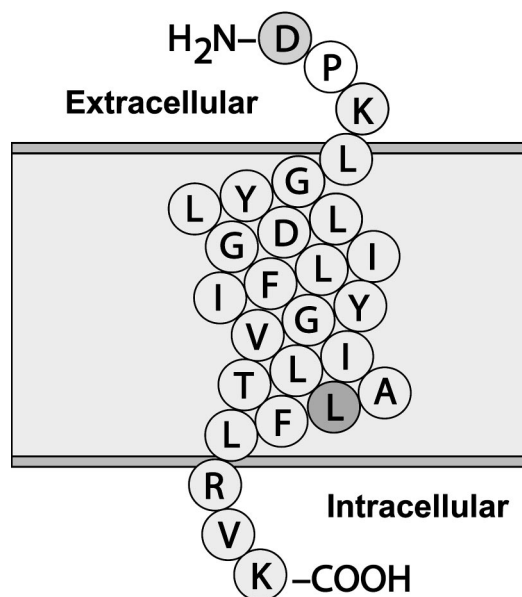
FIG. 1. Schematic representation of the CD3ζ peptide in the membrane bilayer. The $^{13}C\!=\!^{18}O$ labeled 49-Leucine is shown shaded.

Few vibrational modes have been well characterized with two-pulse and three-pulse infrared photon echoes, and even fewer studies have been performed on peptides or protein systems. Of the systems that have been studied, the dephasing of carbon monoxide bound to hemoglobin[29,30] and azide bound to carbonic anhydrase II and hemoglobin are classic cases.[31] More similar to the work presented in this article are the stimulated photon echo experiments on the amide I vibrations of two small globular proteins: apamin and a *de novo* cyclic pentapeptide.[32] In these experiments, fluctuations in the protein backbone were monitored through the amide I band (the carbonyl stretches), and it was found that the first moment of the echo signal decays on a 3–5 ps time scale. In contrast, the first moment of a peptide with only a single amide I mode, N-methylacetamide, decays within 1 ps.[18] These studies illustrate that the amide I line shape contains information on the structure and dynamics of the peptide and its environment.

The CD3ζ membrane peptide is one of the invariant subunits of the T-cell receptor and is essential for T-cell receptor expression.[33–35] The human CD3ζ chain is 163 residues long and its transmembrane segment (residues 31–51), which is α-helical, spans the membrane once (see Fig. 1). Its structure has been studied with multiple site-specific infrared dichroism,[33] in which specific amide I bands along the length of the peptide are spectroscopically isolated using $1-^{13}C\!=\!^{18}O$ isotope labeling and their dichroism is measured in oriented membranes using attenuated total reflection Fourier transform infrared (ATR-FTIR) spectroscopy. The results are consistent with a tetramer transmembrane helical bundle with the helices oriented 12° to the membrane normal. Since the residues of CD3ζ span the width of the membrane, amide I modes near the ends of the peptide are partially solvent exposed and may hydrogen bond to the membrane headgroups, while amide I modes near the center

of the peptide reside in a hydrophobic environment, surrounded by the membrane hydrocarbon chains.

In this paper, we explore whether the heterogeneous environment of the membrane is evident in the linewidths of the peptide amide I modes. Using $1-^{13}C\!=\!^{18}O$ isotope labeling, we probe the vibrational dynamics of a single residue near the end of the peptide and compare the measured dynamics to the line shape of the entire CD3ζ amide I band. We find that this site is much more inhomogeneously broadened than most of the amide I modes in the peptide, suggesting that the vibrational dynamics of the amide I mode might be used to probe the location of residues in membrane-bound peptides.

II. EXPERIMENT

The heterodyned 2D IR spectra were collected using a laser system described in detail previously.[16] In brief, femtosecond mid-IR pulses (1.2 μJ, 150 cm^{-1} bandwidth) were generated by difference frequency mixing the signal and idler beams of a Barium Borate optical parametric amplifier in a AgGaS$_2$ crystal. The pulses were split into three beams k_1, k_2, and k_3 and focused into the sample in a equilateral triangle geometry. The signal was monitored in the $-k_1 + k_2 + k_3$ phase matching direction with a fourth local oscillator pulse that measured the time dependence of the emitted signal in a balanced heterodyne detection system. All four pulses have the same polarizations. The time delay between pulses in the directions $-k_1$ and k_2 is t_1, between k_2 and k_3 is t_2, and between k_3 and the local oscillator pulse is t_3. In the experiments reported here, a two-pulse echo was performed by setting $t_2=0$, and the 2D IR data set was generated by collecting the heterodyned signal as a function of t_3 and t_1, which were both stepped from 0 to 1800 fs in 18-fs steps. The 2D IR spectra were generated by Fourier transforming the time-domain data along t_1 and t_3. Nonresonant signals were not observed.

Isotopically labeled membrane peptide samples were synthesized as described previously.[33] Peptide samples were prepared in dimyristoylphosphatidylcholine (DCMP) with both H$_2$O and D$_2$O as solvent. The H$_2$O sample was prepared using a protocol that produces oriented bilayers.[33] This sample was used to collect the ATR-FTIR spectrum presented below. Since the 2D IR spectra must be collected in transmission geometry, D$_2$O samples were necessary as well. These were prepared by successively dissolving and drying the peptide sample to exchange all of the solvent accessible labile protons. The sample was then placed between two CaF$_2$ plates separated by 56 μm and the concentration of the lipid/D$_2$O solution was varied to adjust the optical density of the absorption bands. The sample prepared in this manner produced unoriented vesicles, as confirmed with polarized transmission FTIR. The linewidths and frequencies of the D$_2$O samples lie within 2 cm^{-1} of the H$_2$O sample, indicating that sample preparation has little effect on the vibrational dynamics.

Because the vesicles range in size from submicron to many microns, the membrane/peptide solution scatters the infrared laser light. Since the purpose of this study is to understand the frequency fluctuations of the biologically rel-

evant segment of the CD3ζ protein, detergents were not used to limit the vesicle size because of the chance that the structure or dynamics of the peptide might be affected by the detergent molecules. Rather, since the scatter was constant over the time scale of the experiment, it was subtracted. For the 2DIR data sets, time scans were collected for each of the axes by setting one of the delays to 1900 fs while scanning the other from 0 to 1800 fs. At 1900 fs, the signal is $<1\%$ of its maximum amplitude, so that the scatter is removed by subtracting the signal for these delays from the two axes of the time-domain data. The scatter was negligible in the transient grating experiment described below.

III. RESULTS

ATR-FTIR and 2D IR spectra were collected for the 28–54 residue segment of the T-cell receptor CD3ζ. The segment is 27 amino acids long and has the sequence DPKLGYLLDGILFIYGVILTA*LFLRVK where *L is the $1-{}^{13}C={}^{18}O$ isotope labeled Leucine at position 49 (49L). In this section, the linear IR, transient grating, and 2D IR spectra of the unlabeled amide I band and the labeled 49-Leucine amide I mode are presented.

A. Linear IR spectrum

The ATR-FTIR spectrum of the peptide in DCMP membranes is shown in Fig. 2. The infrared spectra of peptides can be correlated to the normal modes of the amide unit that form the peptide backbone—e.g., the amide A, I, II, III, etc., modes.[36] The amide I band is primarily due to the carbonyl stretch of the amide unit, while the amide II is largely due to the NH bending and CN stretching motions. These two bands appear at 1656 and 1545 cm^{-1} in Fig. 2, respectively. The other amide bands lie outside of the frequency range probed in the experiments reported here. The band at 1737 cm^{-1} in Fig. 2 is the ester stretch mode of the membrane headgroups. Two smaller peaks also appear in the spectrum at 1594 and 1615 cm^{-1}. The peak at 1594 cm^{-1} is due to the amide I mode of the $^{13}C={}^{18}O$ isotope labeled 49L.[33] Since the ^{18}O labeling procedure is ~80% efficient, not all of the peptides are properly labeled; approximately 20% of the 49L residues are instead $^{13}C={}^{16}O$ labeled and appear at 1615 cm^{1}, along with naturally abundant $^{13}C={}^{16}O$.

B. 2D IR spectrum of the ^{12}C amide I band

The 2D IR spectrum of the unlabeled amide I band was generated from a pulse sequence with $t_2=0$ (e.g., a two-pulse photon echo arrangement) and the absolute value of the 2D IR spectrum is shown in Fig. 3(a). In this spectrum, the center frequency of the laser was set to 1665 cm^{-1} and the bandwidth of the pulses spans the fundamental frequencies of the amide I and membrane headgroup bands. Each of these bands produce a feature in the 2D IR spectrum, centered at $(\omega_1,\omega_3)=(1655 \text{cm}^{-1}, 1653 \text{cm}^{-1})$ and (1720, 1710), respectively. The headgroup band is asymmetric in shape, and the spectra appear to exhibit cross peaks with the amide I band. These observations will be addressed in a later publication. In this paper, we focus on the shape of the amide I band that reflects the distribution of amide I eigenstates in
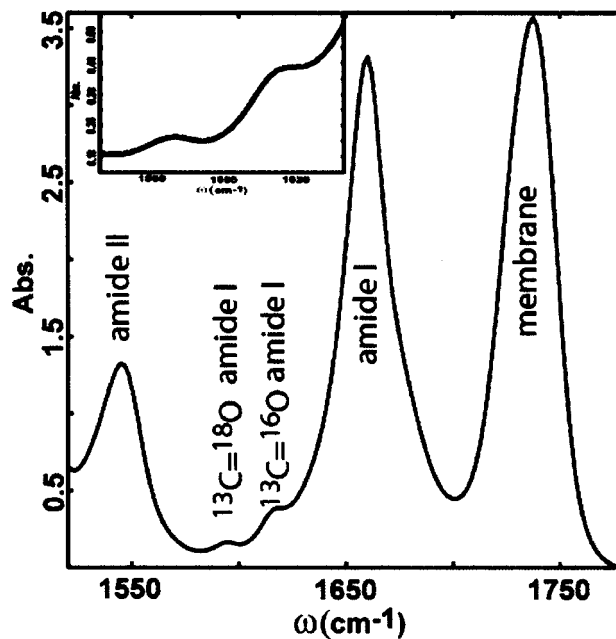

FIG. 2. ATR-FTIR spectrum of CD3ζ. The expanded region of the $^{13}C={}^{18}O$ (1594 cm^{-1}) and $^{13}C={}^{16}O$ (1615 cm^{-1}) labeled amide I mode is shown in the inset.

the helix and the dynamics of the vibrational modes. The photon echo pulse sequence used to collect the 2D IR spectrum eliminates the inhomogeneous width along the antidiagonal.[9,17,18] As a result, homogeneously broadened modes appear round in 2D IR spectra, whereas inhomogeneously broadened modes are elongated along the diagonal. Thus, by simple inspection, it is clear that the amide I band is strongly inhomogeneous.

C. 2D IR spectrum of the $^{13}C={}^{18}O$ labeled 49L

The same two-pulse photon echo pulse sequence used to collect the 2D IR spectrum of the unlabeled amide I band was used on the $^{13}C={}^{18}O$ labeled 49L peak, shown in Fig. 3(b). To generate this spectrum, the center frequency of the infrared pulses was tuned to 1590 cm^{-1}. Now the pulse bandwidth spans the amide II band (1547, 1552), the $^{13}C={}^{18}O$ labeled 49L mode (1596, 1593), and the $^{13}C={}^{16}O$ 49L amide I mode (1624, 1618). Cross peaks also appear in this spectrum. The strongest cross peaks appear between the amide II and amide I modes at (1575, 1547) and (1556, 1586) and indicate that these two modes are coupled. In no case are the cross peaks more than 20% of the intensity of the $^{13}C={}^{18}O$ diagonal peaks. Cross peaks between amide I and II modes have been observed before in a number of peptides.[1,9,11,18] The 2D IR spectrum does not extend above 1630 cm^{-1} because the optical density of the peak increases rapidly as the frequency approaches the unlabeled amide I band, which has an OD of ~3 in this sample at 1655 cm^{-1}. The optical density of the $^{13}C={}^{18}O$ amide I band is ~0.05.

Once again, the inhomogeneous nature of the bands is apparent from the elongation of the 2D IR spectrum. The $^{13}C={}^{18}O$ peak is clearly inhomogeously broadened, whereas the amide II band is more homogeneous in nature. The dynamics of the $^{13}C={}^{16}O$ mode cannot be adequately
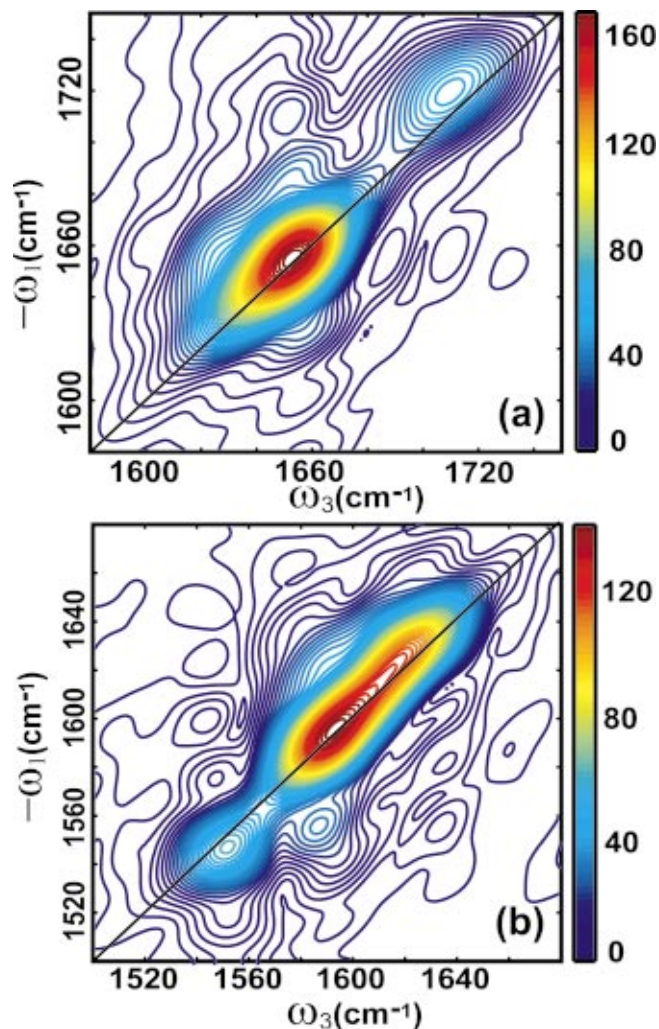
FIG. 3. (Color) 2DIR spectra of the CD3ζ peptide. (a) ^{12}C amide I mode at $(\omega_1, \omega_3) = (1655\ cm^{-1},\ 1653\ cm^{-1})$ and the membrane headgroup at (1720, 1710). (b) $^{13}C={}^{18}O$ amide I mode of 49L is at (1596, 1593), the amide II band is at (1547, 1552), and the $^{13}C={}^{16}O$ 49L amide I mode is at (1624, 1618).

D. Transient grating of the ^{12}C amide I band

A homodyne integrated transient grating experiment was performed on the ^{12}C amide I band in order to determine the characteristic vibrational relaxation time T_{10} of the membrane peptide. The signal is shown in Fig. 4 (solid line) and was collected by setting $t_1 = 0$ and scanning t_2. A biexponential fit (dashed line) to the signal gives time constants of $375(\pm 50)$ and $1150(\pm 50)$ fs with equal contributions. While not as good, a single time constant of 600 fs adequately describes the data.
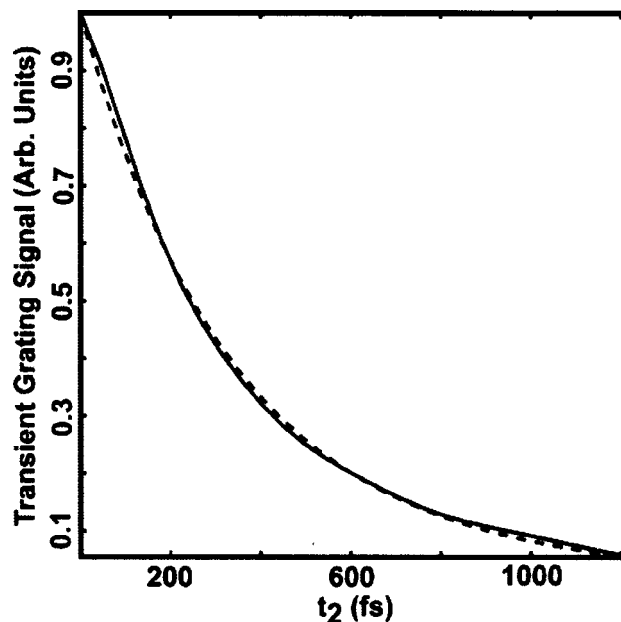
assessed in this spectrum because of the attenuation at higher wave numbers. We emphasize that the $^{13}C={}^{18}O$ peak is now solely due to the labeled 49L residue and is not a band of states like the ^{12}C amide I peak in Fig. 3(a). Thus the 2D line shape of this mode reflects the vibrational dynamics of the single 49L amide I mode.

FIG. 4. Transient grating signal (solid) for the ^{12}C amide I mode of the CD3ζ peptide and biexponential fit (dashed).

IV. DISCUSSION

The 2D line shapes measured in the 2D IR spectra described above depend on the vibrational dynamics, anharmonicities, and distribution of eigenstates of the peptide. These quantities are connected by the molecular potential that includes intramolecular couplings and solvent interactions, among other possible forces. In this section, we outline a Hamiltonian that accounts for intramolecular and intermolecular forces in a general way. We then justify the use of a reduced Hamiltonian to describe the dynamics of the $^{13}C={}^{18}O$ 49L amide I mode and simulate the 2D IR spectrum. Finally, we end this section with a discussion of the structural origins of the vibrational dynamics in the CD3ζ membrane peptide.

A. Modeling the vibrational dynamics of 49L as an isolated oscillator

Vibrational linewidths arise from fluctuations in the frequency of the modes and the energy flow out of the modes.[24,25] In low-temperature gas-phase samples, linewidths are usually dominated by the energy flow, or population relaxation time, of the mode, because few collisions occur that alter the frequencies. In condensed-phase systems, the opposite is often true. Solvated molecules interact strongly with nearby solvent molecules either by collisions, electrostatics, or other mechanisms. In molecules with more than one normal mode, the solvent can indirectly cause frequency fluctuations by acting on vibrational modes coupled to the mode of interest. Of course, structural changes in the molecule can also cause frequency shifts. As a result, the linewidths of condensed-phase modes contain information on the structural and dynamical inhomogeneity of the peptide and its surrounding environment.

The frequency fluctuations responsible for the 49L line shape can have a number of origins. Solvent can directly

influence the amide I energy, by hydrogen bonding, for ex-ample, or indirectly alter the energy through modes coupled to 49L, such as the amide Il and ^{12}C amide I bands. Population relaxation also contributes to the linewidth, which is probably caused by coupling to low-frequency peptide and solvent modes.[8] As a consequence, the Hamiltonian that describes the 49L amide I mode must, in principle, include the entire potential energy surface. We write the one-quantum Hamiltonian[37] in the basis of the individual amide I and amide II local modes as

$$
H = \begin{bmatrix}
E_{49}^{I} - \delta E_{49}^{I} - i\Gamma_{49}^{I} & \alpha_{49,n} - \delta\alpha_{49,n} & \alpha_{49,n+1} - \delta\alpha_{49,n+1} & & \beta_{49,n} - \delta\beta_{49,n} & \\
\alpha_{49,n} - \delta\alpha_{49,n} & E_{n}^{I} - \delta E_{n}^{I} - i\Gamma_{n}^{I} & \alpha_{n,n+1} - \delta\alpha_{n,n+1} & \cdots & \beta_{n,n} - \delta\beta_{n,n} & \cdots \\
\alpha_{49,n+1} - \delta\alpha_{49,n+1} & \alpha_{n,n+1} - \delta\alpha_{n,n+1} & E_{n+1}^{I} - \delta E_{n+1}^{I} - i\Gamma_{n+1}^{I} & & \beta_{n+1,n} - \delta\beta_{n+1,n} & \\
& \vdots & & \ddots & & \\
\beta_{49,n} - \delta\beta_{49,n} & \beta_{n,n} - \delta\beta_{n,n} & \beta_{n+1,n} - \delta\beta_{n+1,n} & & E_{n}^{II} - \delta E_{n}^{II} - i\Gamma_{n}^{II} & \\
& \vdots & & & & \ddots
\end{bmatrix},
\tag{1}
$$

where E_{49}^{I} is the energy of the 49L amide I mode, E_{n}^{I} are the energies of the other 26 amide I sites, E_{n}^{II} are the energies of the amide II sites, δE is the fluctuation in the energies of the sites, α and β are the couplings between the sites, and the fluctuation in the couplings are $\delta\alpha$ and $\delta\beta$. In this Hamiltonian, fluctuations in the hydrogen bonding would introduce diagonal disorder by $\delta E \neq 0$, while fluctuations in the structure would be one cause of off-diagonal disorder with $\delta\alpha \neq 0$ and/or $\delta\beta \neq 0$. Larger conformational fluctuations that are a result of low-frequency modes are considered to contribute to the diagonal disorder through δE. The lower-frequency peptide and solvent modes are contained in $\Gamma = 1/\pi T_{10}$, which accounts for population relaxation.

From Eq. (1) it is clear that the energy of the 49L mode depends on the other modes of the peptide. However, the Hamiltonian for the ^{13}C$=^{18}$O labeled 49L mode can be simplified with two reasonable approximations. First, consider that isotope labeling 49L shifts the fundamental frequency $\sim$60 cm^{-1} from the unlabeled amide I modes. Since experimental[12] and theoretical work[38–40] on the coupling between amide I modes places the largest $\alpha_{49,n}$ at not more than 10 cm^{-1} and probably less than 6 cm^{-1}, frequency fluc-

tuations on E_{n}^{I} will not shift E_{49}^{I} by more than a few wave numbers. Since it is apparent from inspection of both the linear and 2D IR spectra that the fwhm of the ^{13}C$=^{18}$O 49L mode is >30 cm^{-1}, the frequency fluctuations caused by $\alpha_{49,n}$ will only contribute a few percent to the total linewidth. Hence the isotope label isolates the labeled 49L amide I mode from the collective fluctuations of the unlabeled helix amide I modes. Second, 49L is not strongly coupled to the amide II band. The presence of cross peaks in Fig. 3(b) indicate that the amide I of 49L is coupled the amide II band, but the coupling must be weak because the strongest cross peaks are <20% of the intensity of the diagonal peaks. Assuming Lorentzian linewidths, an anharmonicity of 14 cm^{-1} for the amide I mode,[12] and the ratio of the diagonal peak to the cross peak, the coupling is <1.5 cm^{-1}. Thus it appears reasonable that $\beta_{49,n}$ will also only contribute a few percent to the total linewidth.

Since it is unlikely that off-diagonal couplings contributes much to the linewidth, the linewidths must be mostly the result of δE_{49}^{I} and Γ_{49}^{I}. In this situation, it is reasonable to approximate the Hamiltonian in Eq. (1) as partially block diagonal:

$$
H = \begin{bmatrix}
E_{49}^{I} - \delta E_{49}^{I} - i\Gamma_{49}^{I} & 0 & 0 & & 0 & \\
0 & E_{n}^{I} - \delta E_{n}^{I} - i\Gamma_{n}^{I} & \alpha_{n,n+1} - \delta\alpha_{n,n+1} & \cdots & \beta_{n,n} - \delta\beta_{n,n} & \cdots \\
0 & \alpha_{n,n+1} - \delta\alpha_{n,n+1} & E_{n+1}^{I} - \delta E_{n+1}^{I} - i\Gamma_{n+1}^{I} & & \beta_{n+1,n} - \delta\beta_{n+1,n} & \\
& \vdots & & \ddots & & \\
0 & \beta_{n,n} - \delta\beta_{n,n} & \beta_{n+1,n} - \delta\beta_{n+1,n} & & E_{n}^{II} - \delta E_{n}^{II} - i\Gamma_{n}^{II} & \\
& \vdots & & & & \ddots
\end{bmatrix}.
\tag{2}
$$

We cannot eliminate the possibility that the energy fluctuations of some peptide mode outside the 100-cm^{-1} region of frequency space probed in these experiments influences the 49L amide I energy, but it seems unlikely considering the large energy difference. Very-low-frequency torsional modes are responsible for peptide conformational changes, and the amide I site energy depends on the peptide structure dihedral angles,[38] but these structural changes are so slow that we consider them static and include them in the diagonal disorder δE_{49}^{I}, as stated above. Thus, in the remaining subsections, we treat the labeled 49L as isolated from the other modes of the helix.

B. Fit to the 2D IR spectrum

Having established that $^{13}C={}^{18}O$ isotope substitution isolates the amide I vibration, we model the amide I mode of 49L as a single oscillator. Assuming Gaussian frequency fluctuations and a linear response, the linear infrared line shape for a single oscillator is given by[24,26,41]

$$I(\omega)=\left(|\mu_{01}|^2\int_{-\infty}^{\infty}e^{-i(\omega-\omega_{10})t-g(t)-|t|/2T_{10}}dt\right), \quad (3)$$

where

$$g(t)=\int_0^t dt'\int_0^{t'}dt''\langle\delta\omega_{10}(t'')\delta\omega_{10}(0)\rangle, \quad (4)$$

μ_{01} is the amide I transition dipole, T_{10} is the vibrational lifetime, ω_{01} is the average frequency of the mode, and $\delta\omega_{01}$ is the instantaneous frequency fluctuation of the mode away from the average. In the homogeneous case, the frequency–frequency correlation function $\langle\delta\omega_{10}(t'')\delta\omega_{10}(0)\rangle$ decays very quickly and the oscillator vibrates with the time-averaged frequency. In the strictly inhomogeneous case $\langle\delta\omega_{10}(t'')\delta\omega_{10}(0)\rangle$ does not decay, resulting in a distribution of frequencies. In between these two limits, the inhomogeneous distribution evolves with time in a process known as spectral diffusion.

While the line shapes of linear spectra contain the desired information on $\langle\delta\omega_{10}(t'')\delta\omega_{10}(0)\rangle$, quantitatively extracting the time scales from the linear spectra is not practical, because very different dynamics can sometimes cause only subtle differences in line shape. More useful approaches are two- and three-pulse photon echo spectroscopies that are valuable tools for accurately measuring the frequency–frequency correlation function.[26] In photon echo spectroscopy, the dynamics is more apparent because inhomogeneous dynamics can be caused to rephase, creating a photon echo. For example, in stimulated photon echo spectroscopy, three pulses hit the sample as described in the experimental section. In the rephasing pulse sequence, the third pulse k_3 reverses the coherence created by the first pulse k_1, which gives rise to the echo. If the system is homogeneous or the inhomogeneous distribution is dynamic, the signal does not rephase or is only partially rephased due to loss in phase memory. By increasing the delay between k_1 and k_2—e.g., t_2—the loss of phase memory is measured, revealing the amount of spectral diffusion. Thus, when the frequency fluctuations occur on two widely varying time scales—e.g., as homogeneous and inhomogeneous broadening—two-pulse photon echoes are sufficient.

Since we used a two-pulse photon echo pulse sequence to collect the 49L 2D IR spectrum, the amide I mode inhomogeneity is removed from the spectrum along the antidiagonal. As a result, by fitting the line-narrowed spectrum, we extract the vibrational time scales. To accomplish this, we have modeled the 2D IR spectrum with a correlation function that consists of an exponential decay and a static offset:

$$\langle\delta\omega(t'')\delta\omega(0)\rangle=\Delta_1^2e^{-t''/\tau_1}+\Delta_0^2, \quad (5)$$

where Δ_0 accounts for the static inhomogeneity of the mode. Δ_1 and τ_1 describe an evolving inhomogeneous distribution,

which is in the homogeneous limit when $\Delta_1\tau_1\ll1$. Using an analogous approach as described above for the linear spectrum, the 2D IR spectrum is calculated by Fourier transforming the third-order response, which is given by

$$S(\omega_3,\omega_1)=\int_{-\infty}^{\infty}\int_{-\infty}^{\infty}e^{-i(\omega_1t_1+\omega_3t_3)}2|\mu_{10}|^4e^{-i\omega_{10}(t_3-t_1)}$$
$$\times(e^{-(t_1+t_3)/2T_{10}}-e^{-(t_1+3t_3)/2T_{21}+i\Delta t_3})$$
$$\times e^{-2g(t_1)-2g(t_3)+g(t_1+t_3)}dt_1dt_3 \quad (6)$$

in the limit of δ-function infrared pulses. The form of $g(t)$ is given in Eqs. (4) and (5). In this equation, the population relaxation times of the $v=1-0$ and $v=2-1$ states are given by T_{10} and T_{21}. Here T_{10} was set to 600 fs in the fits, while $T_{21}=400$ fs, which follows from the ratio of T_{10} to T_{21} measured for N-methylacetamide.[18] The anharmonicity is $\Delta=14$ cm^{-1} as determined recently for a soluble helical peptide.[12] The variables Δ_1, τ, and Δ_0 in Eq. (5) were varied until the simulation and signal agreed. Because the 49L amide I band overlaps with the amide II and $^{13}C={}^{16}O$ amide I bands, our fit also includes 2D line shapes for these modes as well. These modes were simulated with 2D IR line shapes that followed the same functional form as Eq. (5), but we do not consider their parameters meaningful since the amide II band at 1550 cm^{-1} includes all of the amide oscillators in the helix whereas the $^{13}C={}^{16}O$ amide I band is attenuated on the high-energy side by the sample OD.

The simulated absolute value 2D IR spectrum obtained from the fit is shown in Fig. 5(a). In Figs. 6(a) and 6(b), slices along the diagonal and antidiagonal of the 2D IR spectrum are shown for the experiment (solid line) and simulation (dashed line). The parameters used in the fit for the $^{13}C={}^{18}O$ amide I mode of 49L are given in Table I, and the 2D IR spectrum of just this mode is simulated in Fig. 5(b). The inhomogeneous nature of the 49L amide I mode is clearly reproduced by these parameters as observed in the elongated amide I mode of the simulated 2D IR spectra. The fit parameters give a static offset of $\Delta_0=2.54(\pm0.07)$ ps^{-1} and the exponential decay falls in the homogeneous limit with $\Delta_1\tau_1=0.01$ ($\Delta_1=4.00$ ps^{-1}, $\tau_1=6$ fs from the fits). Since $\Delta_1\tau_1\ll1$, the pure dephasing time is given by $T_2^*=(\Delta_1^2\tau_1)^{-1}=10\pm3$ ps. T_2^* is better determined than either Δ_1 or τ_1 individually, because the 2DIR spectrum measures the homogeneous linewidth. Using Eq. (3) and the parameters in Table I, the T_{10} time contributes 9 cm^{-1} to the 49L linewidth [calculated by $(1/2\pi cT_{10})$], T_2^* contributes 2 cm^{-1} (calculated by $1/\pi cT_2$), and 32 cm^{-1} comes from the inhomogeneous distribution, where c is the speed of light. Including finite pulse widths and nonrephasing processes in the fits changes the linewidth by less than 1 cm^{-1}.

Both two-pulse- and three-pulse-stimulated photon echoes have been used to monitor the vibrational dynamics of infrared modes.[28,30] In low-temperature glasses and solids the dynamics may lie in the Bloch limit, in which case the inhomogeneous distribution is fixed and two-pulse photon echoes are sufficient to quantify the timescales. Molecular vibrations in room-temperature liquids do not generally lie in the Bloch limit, and we expect that some portion of the in-
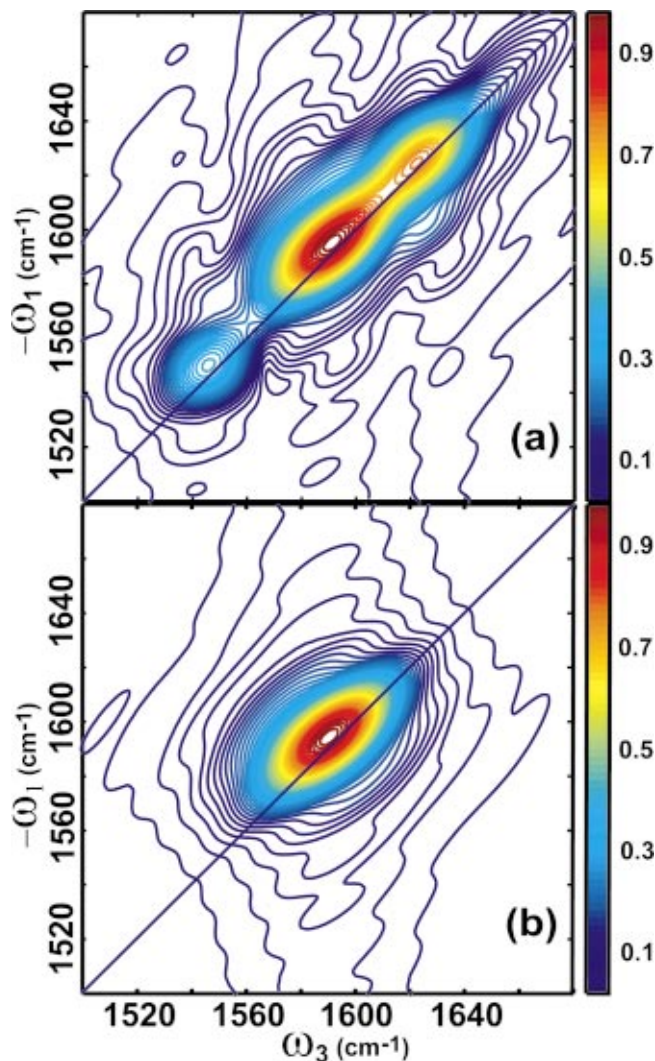
FIG. 5. (Color) (a) Fit to the 49L 2D IR spectrum shown in Fig. 3(b). (b) Simulated 2D IR spectrum of just the 49L ^{13}C $=^{18}$O amide I mode using the parameters listed in Table I.
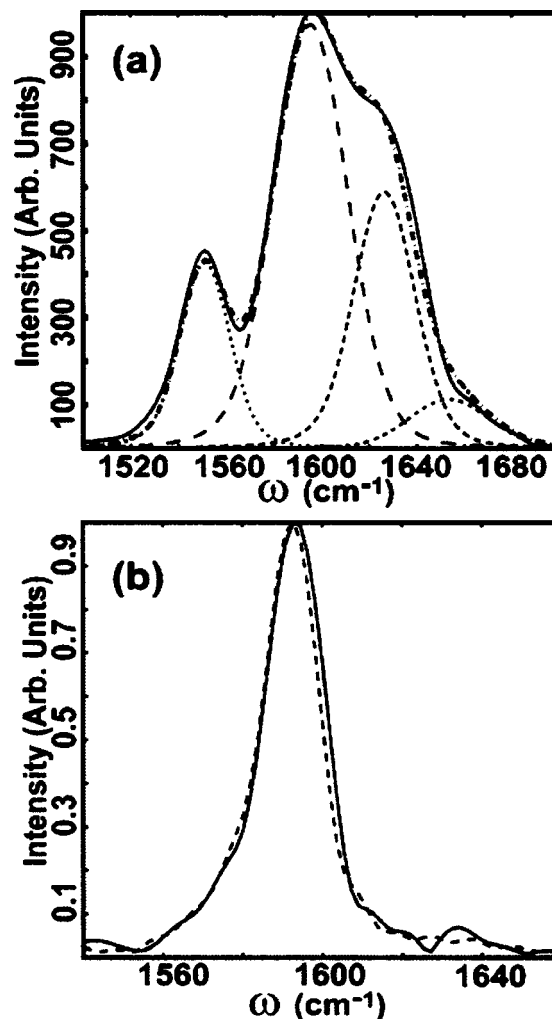

FIG. 6. (a) Diagonal slice ($\omega = \omega_1 = \omega_3$) of the experimental 49L 2D IR spectrum (solid line) and the simulated fit (dot-dashed line). Also shown is the contribution of the ^{13}C $=^{18}$O 49L line shape (dashed line). The other contributions are from the amide II and the attenuated amide I bands (dotted). (b) Antidiagonal slice of the experimental (solid line) and the simulated (dashed line) 2D IR spectra taken through the peak maximum of the ^{13}C $=^{18}$O amide I band.

homogeneous distribution, accounted for by the static offset in Table I, may spectrally diffuse. Spectral diffusion has been observed on the amide I bands of some soluble peptides using stimulated echoes,[32] but it was not clear whether the observed spectral diffusion was due to the dynamic inhomogeneity of the sites or to structural changes causing diffusion of the exciton frequencies. The isotope labeling approach used here should be able to address this issue, but unfortunately it was not possible to perform an integrated three-pulse photon echo on the CD3ζ peptide because of scattering from the sample. 2D IR spectroscopy could still be used to detect and quantify the spectral diffusion of the isotope labeled residue by monitoring the 2D line shape as a function of t_2 time.[42,43] This approach will be used at a later date to obtain the time scales for a generalized Kubo model.[49]

C. Comparison to the ^{12}C mode

In the previous subsection, the correlation function for a single-site amide I mode in the helix was determined. The question remains as to whether the dynamics of this particu-

lar site is representative of all the sites in the helix. On the one hand, it might be expected that the highly helical nature of the CD3ζ peptide would lead to similar dynamics throughout the length of the helix, but on the other hand, the helix terminates at the surface of the membrane and some number of residues at the end of the peptide must be exposed to solvent and the membrane headgroups. To explore these issues, we compare the line shape of the 49L residue to the amide I band of the helix. Using the parameters given in Table I and Eqs. (3)–(5), the line shape of the 49L amide I mode is simulated in Fig. 7 and plotted against the experimental linear spectrum of the ^{12}C amide I band. The 49L amide I has a full width at half maximum (FWHM) of 35

TABLE I. Parameters used to fit the ^{13}C $=^{18}$O amide I mode of 49-Leucine.

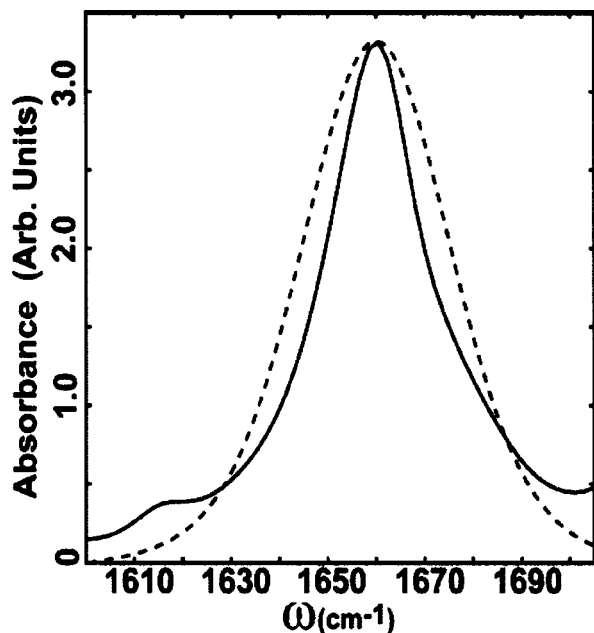| ω	Δ	T_{10}	T_{21}	T_2^*	Δ_0
1595 cm^{-1}	14 cm^{-1}	600 fs	400 fs	10±3 ps	2.54±0.07 ps^{-1}

FIG. 7. Comparison of the experimental ATR-FTIR line shape of the ^{12}C amide I band (solid line) to the simulated linear spectrum of 49L (dashed line) using the parameters in Table I.

cm^{-1}, 9 cm^{-1} wider than the unlabeled ^{12}C amide I band (26 cm^{-1} fwhm). Furthermore, the diagonal width of the ^{13}C=^{18}O band is wider than the C=O band in the 2DIR spectra (Fig. 3). In this section we develop a model to qualitatively interpret the line shape of the ^{12}C=^{16}O for comparison to labeled amide linewidth.

Since 49L is modeled as an independent oscillator, its line shape is straightforward to interpret. Interpretation of the ^{12}C amide I linewidth is not as clear cut because the coupling between the ^{12}C amide I modes cannot be neglected. As a result, the observed infrared transitions are the collective oscillations of many individual amide I vibrations and therefore must depend on the vibrational dynamics at each of these sites. The one-quantum Hamiltonian for a perfectly ordered helix, written in the individual amide I site basis, is given by

$$
H = \begin{bmatrix} E - \delta E_1 - i\Gamma & \alpha_1 & \alpha_2 & \\ \alpha_1 & E - \delta E_2 - i\Gamma & \alpha_1 & \cdots \\ \alpha_2 & \alpha_1 & E - \delta E_3 - i\Gamma & \\ & \vdots & & \ddots \end{bmatrix}.
\tag{7}
$$

Equation (7) is a special case of the general Hamiltonian described by Eq. (1). In a perfect helix, the coupling terms in the Hamiltonian are periodic because of the helical symmetry. Furthermore, the amide I modes are all equivalent and thus have identical frequencies E. Since we are interested in how the frequency fluctuations of the individual sites affect the exciton modes of the helix, we allow each site to have its own fluctuation δE_n. For the sake of simplicity, we consider identical linewidths Γ and, based on our arguments above, we neglect the effects of coupling to the amide II and other peptide modes—i.e., $\beta_{n,m} = 0$ in Eq. (2).

We identify two limits for the above Hamiltonian. First, we consider the case where the dynamics is homogeneous in nature. In this case, the frequency fluctuations are very fast, and the frequency correlation function is a rapidly decaying function. As a result, $\delta E_n \sim 0$, the linewidth is dominated by the linewidth Γ, and the Hamiltonian becomes

$$
H = \begin{bmatrix} E & \alpha_1 & \alpha_2 & \\ \alpha_1 & E & \alpha_1 & \cdots \\ \alpha_2 & \alpha_1 & E & \\ & \vdots & & \ddots \end{bmatrix} - i\Gamma(\underset{\approx}{I}),
\tag{8}
$$

where $\underset{\approx}{I}$ is the identity matrix. Due to the periodic nature of the Hamiltonian, the bracketed term has an analytical solution for an infinite helix.[44–46] By symmetry, an infinite helix only has three allowed infrared transitions: one transition that is parallel to the helix axis and two degenerate modes that are perpendicular to the helix axis. These give the A and E bands, respectively. For α-helices, the intensity of the parallel mode is much stronger than the perpendicular modes because the angle of the amide I transition dipoles lie nearly parallel to the helix axis. Moreover, the wave functions of the modes are given by

$$
|\Psi_\parallel\rangle = \sum_n \frac{1}{\sqrt{N}} |\phi_n\rangle
\tag{9a}
$$

and

$$
|\Psi_\perp\rangle = \sum_n \frac{1}{\sqrt{N}} \exp(2\pi i n/3.6) |\phi_n\rangle,
\tag{9b}
$$

where $|\phi_n\rangle$ are the individual local-mode amide I sites corresponding to a single quantum of excitation, N is the number of amide I sites, and 3.6 is the number of residues per turn of an α-helix. The energies of the parallel and perpendicular bands are given by

$$
E_\parallel = E + \sum_n \alpha_{1,n},
\tag{10a}
$$

$$
E_\perp = E_0 + \sum_n \alpha_{1,n} \cos(2\pi n/3.6).
\tag{10b}
$$

According to Eqs. (9a) and (9b), the individual amide I sites all contribute equally to the exciton wave functions. The only difference between the parallel and perpendicular modes is the relative phases of the amide I sites. As a result, the A- and E-allowed transitions, which are the dominant features in the infrared spectrum of an well-formed α-helix, have the same linewidth, given by Γ. If the sites have different linewidths Γ_n, an average lifetime would be measured.

In the second limit, we consider the situation when the fluctuations in the site energies δE_n are much greater than the coupling α_n. In this case, the frequency shifts caused by off-diagonal disorder are neglible compared to the disorder created by inhomogeneities of the sites, and the Hamiltonian reduces to

$$H = \begin{bmatrix} E - \delta E_1 - i\Gamma & 0 & 0 & \\ 0 & E - \delta E_2 - i\Gamma & 0 & \cdots \\ 0 & 0 & E - \delta E_3 - i\Gamma & \\ & \vdots & & \ddots \end{bmatrix}.$$

(11)

Thus diagonal disorder localizes the vibrational energy onto the sites.[47] The observed amide I linewidth would then be an average of the inhomogeneities of the individual sites, convoluted with the population relaxation time.

We know from our fits to the 2D IR spectrum that the 49L mode is largely inhomogeneously broadened, the inhomogeneity accounting for 32 cm^{-1} of the width in the linear spectrum (Table I). This amount of inhomogeneity is much larger than the coupling typically observed in helical peptides (<10 cm^{-1}; see discussion above). As a result, if 49L were representative of all the sites in the helix, the Hamiltonian for the helix would be described by Eq. (11) and the line shape of the ^{12}C amide I band would be as wide as the amide I of 49L. This is clearly not the case: the ^{12}C amide I band in Fig. 7 is much narrower than 49L. Furthermore, delocalized wave functions would not be possible if the inhomogeneity of 49L were typical for all the sites in the peptide, but other experiments find that the amide I band of α-helical peptides is significantly delocalized.[8,48] Therefore, it is more likely that most of the amide I sites are much more homogeneous than 49L and that delocalized excitonic wave functions may still exist in other regions of the helix. Whether or not this is the case, 49L cannot participate in delocalization because of its large site disorder even when it is unlabeled.

Regardless of the dynamics at 49L, the excitonic wave functions described by Eq. (9) might still exist over the remaining amide I modes, depending on the magnitudes of the frequency fluctuations at the remaining sites. Since the amide I linewidth is 35 cm^{-1}, and 9 cm^{-1} of this comes from the Γ, it is reasonable to believe that site disorder in other parts of the helix is more comparable to the coupling strengths. Further isotope labeling studies are necessary to explore these possibilities.

D. Structural origin of the vibrational linewidths

Membrane peptides reside in a very heterogeneous environment. In helical transmembrane peptides like CD3ζ, the helix terminates at the surface of the membrane where it can hydrogen bond with the membrane headgroups and may be partially exposed to the solvent. In contrast, the residues of the helix that lie in the center of the membrane bilayer only interact with the hydrophobic hydrocarbon chains. In this region, water is excluded from the membrane and hydrogen bonds do not form between the peptide and membrane. As a result, the environment surrounding the helix and the helix itself are considerably different for residues in the center than near the surface of the membrane.

Considering the above factors, we expect the vibrational dynamics to be very different for amide I modes near the surface of the membrane than those present in the middle. This is consistent with our observations. 49L lies in the first turn of the helix (Fig. 1), near the membrane headgroups, whereas the majority of ^{12}C amide I modes lie in the hydrophobic region of the membrane. Considering that the site disorder δE_n is largely due to hydrogen bonding, it appears reasonable that 49L is more inhomogeneously broadened than the majority of the amide I site modes. Work is currently underway on ten other ^{13}C$=\!^{18}$O labeled amide I residues to test this hypothesis and characterize the vibrational dynamics along the entire length of the helix.

V. CONCLUSION

Using a combination of $1-^{13}$C$=\!^{18}$O isotope labeling and heterodyned 2D IR spectroscopy, we have measured the homogeneous and inhomogeneous linewidths of a single amide I mode (49-Leucine) of the transmembrane segment of the CD3ζ protein reconstituted in lipid vesicles. We believe that this is the first 2D IR study of a membrane bound peptide. By fitting the photon echo 2D IR spectrum, we find that the linewidth of the 49-Leucine amide I mode is mostly due to inhomogeneous broadening. Comparison of the 49-Leucine amide I mode to the amide I band of the entire 27-residue peptide suggests that the amide I modes of the majority of residues in the peptide are more homogeneous than 49-Leucine, possibly because the interior of the membrane is hydrophobic and does not hydrogen bond to the peptide. If this is true, then it may be possible to determine the depth of residues in membrane bilayers by the 2D line shapes of isotopically labeled residues. Since traditional structural techniques like x-ray crystallography and NMR spectroscopy are much more difficult to apply to membrane proteins than they are to soluble proteins, developing alternative techniques to probing the structures and dynamics of membrane systems is of the utmost importance.

[1] M. T. Zanni, N.-H. Ge, Y. S. Kim, and R. M. Hochstrasser, Proc. Natl. Acad. Sci. U.S.A. **98**, 11265 (2001).
[2] M. Khalil, N. Demirdöven, and A. Tokmakoff, J. Phys. Chem. A **107**, 5258 (2003).
[3] K. A. Meyer, D. M. Besemann, and J. C. Wright, Chem. Phys. Lett. **381**, 642 (2003).
[4] N.-H. Ge, M. T. Zanni, and R. M. Hochstrasser, in *Ultrafast Phenomena XIII*, edited by N. S. M. M. Murnane, R. J. D. Miller, and A. M. Weiner (Springer-Verlag, Berlin, 2004), p. 592.
[5] S. Yeremenko, M. S. Pshenichnikov, and D. A. Wiersma, Chem. Phys. Lett. **369**, 107 (2003).
[6] J. B. Ashbury, T. Steinel, C. Stromberg, K. J. Gaffney, I. R. Piletic, A. Goun, and M. D. Fayer, Chem. Phys. Lett. **374**, 362 (2003).
[7] C. J. Fecko, J. D. Eaves, J. J. Loparo, A. Tokmakoff, and P. L. Geissler, Science **301**, 1698 (2003).
[8] P. Hamm, M. Lim, and R. M. Hochstrasser, J. Phys. Chem. B **102**, 6123 (1998).
[9] M. T. Zanni, S. Gnanakaran, J. Stenger, and R. M. Hochstrasser, J. Phys. Chem. B **105**, 6520 (2001).
[10] S. Woutersen and P. Hamm, J. Chem. Phys. **115**, 7737 (2001).

[11] M. T. Zanni and R. M. Hochstrasser, Curr. Opin. Struct. Biol. **11**, 516 (2001).

[12] C. Fang, J. Wang, A. K. Charnley, W. Barber-Armstrong, A. B. Smith III, S. M. Decatur, and R. M. Hochstrasser, Chem. Phys. Lett. **382**, 586 (2003).

[13] A. T. Krummel, P. Mukherjee, and M. T. Zanni, J. Phys. Chem. B **107**, 9165 (2003).

[14] A. Piryatinski, S. Tretiak, V. Chernyak, and S. Mukamel, J. Raman Spectrosc. **31**, 125 (2000).

[15] O. Golonzka, M. Khalil, N. Demirdöven, and A. Tokmakoff, Phys. Rev. Lett. **86**, 2154 (2001).

[16] E. C. Fulmer, P. Mukherjee, A. T. Krummel, and M. T. Zanni, J. Chem. Phys. **120**, 8067 (2004).

[17] A. Tokmakoff, J. Phys. Chem. A **104**, 4247 (2000).

[18] M. T. Zanni, M. C. Asplund, and R. M. Hochstrasser, J. Chem. Phys. **114**, 4579 (2001).

[19] S. Ham, J.-H. Kim, H. Lee, and M. Cho, J. Chem. Phys. **118**, 3491 (2003).

[20] D. E. Thompson, K. A. Merchant, and M. D. Fayer, J. Chem. Phys. **115**, 317 (2001).

[21] N.-H. Ge, M. T. Zanni, and R. M. Hochstrasser, J. Phys. Chem. A **106**, 962 (2002).

[22] N. Demirdoven, M. Khalil, and A. Tokmakoff, Phys. Rev. Lett. **89**, 237401/1 (2002).

[23] R. Venkatramani and S. Mukamel, J. Chem. Phys. **117**, 11089 (2002).

[24] R. Kubo, Adv. Chem. Phys. **15**, 101 (1969).

[25] J. Chesnoy and G. M. Gale, Adv. Chem. Phys. **70**, 297 (1988).

[26] S. Mukamel, *Principles of Nonlinear Spectroscopy* (Oxford University Press, New York, 1995).

[27] M. C. Asplund, M. T. Zanni, and R. M. Hochstrasser, Proc. Natl. Acad. Sci. U.S.A. **97**, 8219 (2000).

[28] P. Hamm, M. Lim, and R. M. Hochstrasser, Phys. Rev. Lett. **81**, 5326 (1998).

[29] K. D. Rector, C. W. Rella, J. R. Hill, A. S. Kwok, S. G. Sligar, E. Y. P. Chien, D. D. Dlott, and M. D. Fayer, J. Phys. Chem. B **101**, 1468 (1997).

[30] K. A. Merchant, Q.-H. Xu, D. E. Thompson, and M. D. Fayer, J. Phys. Chem. A **106**, 8839 (2002).

[31] M. Lim, P. Hamm, and R. M. Hochstrasser, Proc. Natl. Acad. Sci. U.S.A. **95**, 15315 (1998).

[32] P. Hamm, M. Lim, W. F. DeGrado, and R. M. Hochstrasser, J. Phys. Chem. A **103**, 10049 (1999).

[33] J. Torres, J. A. G. Briggs, and I. T. Arkin, J. Mol. Biol. **316**, 365 (2002).

[34] N. Manolios, Immunol. Cell Biol. **73**, 544 (1995).

[35] H. Jacobs, Immunol. Today **18**, 565 (1997).

[36] S. Krimm and J. Bandekar, Adv. Protein Chem. **38**, 181 (1986).

[37] T. Uzer and W. H. Miller, Phys. Rep. **199**, 73 (1991).

[38] H. Torii and M. Tasumi, J. Chem. Phys. **96**, 3379 (1993).

[39] H. Torii and M. Tasumi, J. Raman Spectrosc. **29**, 81 (1997).

[40] P. Hamm and S. Woutersen, Bull. Chem. Soc. Jpn. **75**, 985 (2002).

[41] D. W. Oxtoby, D. Levesque, and J.-J. Weis, J. Chem. Phys. **68**, 5528 (1978).

[42] J. B. Asbury, T. Steinel, G. Stromberg, K. J. Gaffney, I. R. Piletic, A. Goun, and M. D. Fayer (unpublished).

[43] M. Khalil, N. Demirdöven, and A. Tokmakoff, Phys. Rev. Lett. **90**, 047401 (2003).

[44] P. W. Higgs, Proc. R. Soc. London, Ser. A **220**, 472 (1953).

[45] W. Moffitt, J. Chem. Phys. **25**, 467 (1956).

[46] T. Miyazawa, J. Chem. Phys. **32**, 1647 (1960).

[47] J. L. Skinner, J. Phys. Chem. **98**, 2503 (1994).

[48] J. Edler and P. Hamm, J. Chem. Phys. **117**, 2415 (2002).

[49] J. R. Schmidt, N. Sundlass, J. L. Skinner, Chem. Phys. Lett. **378**, 559 (2003).